Technical Paper
Int'l J. of Aeronautical & Space Sci. 12(4), 331–345 (2011)
DOI:10.5139/IJASS.2011.12.4.331

IJASS
International Journal of Aeronautical and Space Sciences

Flutter Control of a Lifting Surface via Visco-Hysteretic Vibration Absorbers

Walter Lacarbonara* and Marek Cetraro**

Department of Structural Engineering, SAPIENZA University of Rome, via Eudossiana, 18 Rome, Italy 00184

Abstract

In this paper, a visco-hysteretic vibration absorber (VA) is proposed to increase the flutter speed of an airfoil and enhance damping in the pre- and post-flutter regimes. The passive system consists of a parallel arrangement of a dashpot and a rate-independent hysteretic element, represented by the Bouc-Wen differential model. The equations of motion are obtained and various tools of linear and nonlinear dynamics are employed to study the effects of the visco-hysteretic VA in the pre- and post-flutter ranges.

Key words: Visco-hysteretic vibration absorber, Flutter control

1. Introduction

Flutter refers to a serious aeroelastic instability in both civil and military aircrafts. The flutter phenomenon is characterized by limit-cycle oscillations (LCOs) of relatively high amplitude, exhibiting several harmonics. Modern fighter airplanes often carry many types and combinations of external wing-mounted stores to satisfy multi-mission requirements. Such stores can reduce the flutter speed and thereby degrade the operational and mission effectiveness of combat airplanes. Due to the importance of flutter avoidance, considerable research has been conducted in the last decades to develop and assess the capabilities of various flutter control concepts (Marzocca et al., 2002; Njuguna, 2007). In the general context of studies on semi-active/active methodologies, an important aspect is associated with the spatial optimization of actuator and sensor parameters to facilitate control of targeted modes while providing roll-off of higher-order modes without the need for phase-inducing filters. In contrast, the complexity inherent in semi-active/active strategies for flutter control is dramatically reduced in passive systems such as VAs. Further, these systems exhibit desirable fault-tolerance characteristics.

A passive flutter control approach, known as the decoupler pylon, has been presented by Reed et al. (1980). The decoupler pylon isolates dynamically the wing from the store pitch inertia effects by means of soft-spring/damper elements assisted by a low-frequency feedback-control system that minimizes static pitch deflections of the store due to maneuvers and changing flight conditions. Wind-tunnel tests and analyses show that this relatively simple pylon suspension system provides substantial increases in flutter speed and reduces the sensitivity of flutter to changes in store inertia and center of gravity. The flutter characteristics of F-16 and F-17 flutter models equipped with decoupler pylon mounted stores are presented by Reed et al. (1980) and compared with results obtained on the same model configurations with active flutter control systems.

A semi-active flutter control strategy for high-aspect-ratio wings has been presented by Hu and Zhou (2007), where multiple magneto-rheological dampers are proposed. In their work, the results of the semi-active approach are contrasted with those obtained by the passive flutter control methodology based on multiple visco-elastic vibration absorbers (VAs).

A design methodology for optimized flutter control

* Email: walter.lacarbonara@uniroma1.it
** Graduate student

Received: October 10, 2011 Accepted: November 29, 2011

http://ijass.or.kr pISSN: 2093-6742 eISSN: 2093-2480

of an aeroelastic delta wing is presented by Richard and Clark (2003). These experiments, employing optimized piezoelectric transducers, show substantially increased flutter control authority over non-optimized systems. They also point out the importance of this spatial coupling as well as the transducer mass and stiffness effects. Works related to semi-active techniques can be found in Schweiger et al. (1999), McGowan (1999), and Rocha et al. (2007), while Njuguna (2007) presents a good review of existing techniques.

In the last century, nonlinear VAs have been proposed by purposeful introduction of nonlinearities in either stiffness or damping. This nonlinearity can be associated with various aspects of the VA restoring force. For example, according to Lee et al. (2007a, b) the flutter and post-flutter control of a two-degree-of-freedom (two-dof) system is realized by a single-dof nonlinear energy sink (NES), which exhibits a nonlinear restoring force without the linear stiffness term. The benefit of this kind of VA lies in its ability to enhance the flutter speed or stabilize the post-flutter LCOs, depending on the initial conditions, flow speed, and mass ratio. Three different control phenomenologies can be seen in the NES, and these are related to the different interactions of the NES with the pitch and heave modes of the two-dof airfoil. In the first case, intermittent action of the NES results in intermittent oscillations of the three-dof system, and thus flutter is not completely suppressed. In the second case, flutter is completely suppressed, while in the third case, stable LCOs arise in the post-flutter range. The results of this study, corroborated by experiments, showed a maximum increase of the flutter speed by 26 per cent.

With regard to material nonlinearities in the VA, Carpineto et al. (2010, 2011) and Vestroni et al. (2011) exploit the hysteresis exhibited by short wire ropes under flexure to engineer a hysteretic VA for passive control of mechanical vibrations. In order to show the effectiveness of the proposed hysteretic VA, Carpineto et al. (2010, 2011) carry out a semi-analytical/numerical and experimental study of a simply supported beam equipped with the hysteretic VA, subject to harmonic and white Gaussian noise base motions.

In this work, a visco-hysteretic VA is investigated for flutter control of a thin airfoil with a careful unfolding of its nonlinear features in the pre- and post-flutter regime.

2. The Governing Equations of Motion

Studies of the flutter condition are often carried out considering a two-dof model of a wing treated as a lifting surface or a thin airfoil, accounting for the plunge and pitch degrees of freedom (Fig. 1). The flutter control strategy of this model is based on incorporation of a VA, located at a distance ηb in the chord-wise direction, which can oscillate

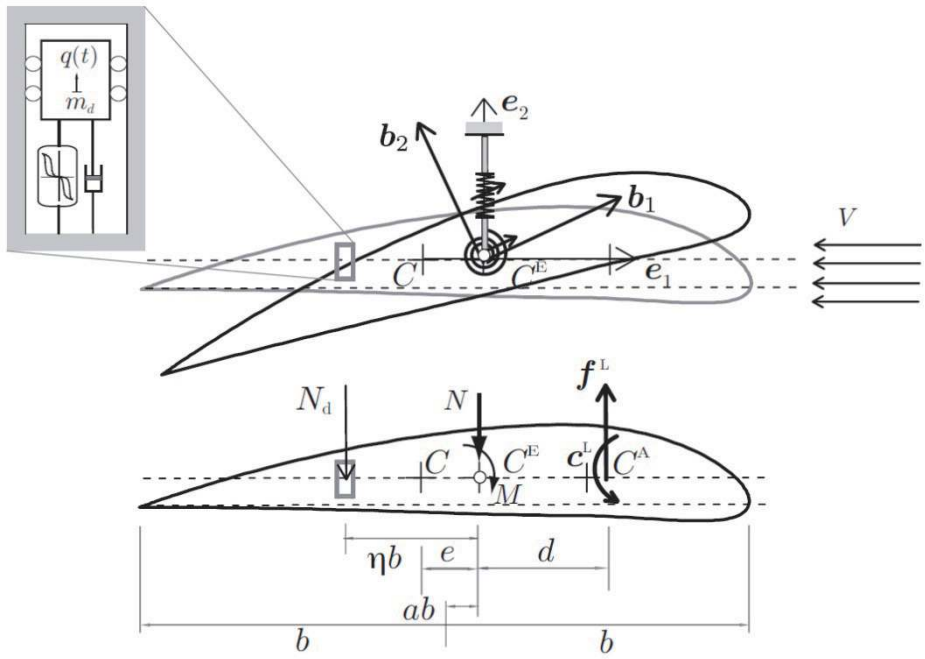

Fig. 1. Lifting surface with the coordinate frame (top) and free-body diagram of the forces (bottom). The main system is augmented by the visco-hysteretic vibration absorber shown in the enlarged box (left).

DOI:10.5139/IJASS.2011.12.4.331

by a displacement q normal to the chord-wise direction (Fig. 1). Here, b represents half the chord length. From this, it can be seen that the augmented system is in fact a three-dof system.

Let $(\boldsymbol{e}_1, \boldsymbol{e}_2)$ be a fixed basis with $\boldsymbol{e}_1$ collinear with the chord-wise direction in the wing's stress-free configuration, while $(\boldsymbol{b}_1, \boldsymbol{b}_2)$ are body-fixed unit vectors rotated in the current configuration by an angle denoted by $\alpha(t)$ (Fig. 1) so that the (counter-clockwise) angle α denotes the pitch degree of freedom. In the stress-free configuration, the origin of the fixed frame is taken coincident with the elastic center C^E, while the center of mass and the aerodynamic center are denoted by C and C^A, respectively. The position vector of a material point that occupies position $\boldsymbol{x}$ in the stress-free configuration of the surface is described in the current configuration by $\boldsymbol{r} = \boldsymbol{r}^C + \check{\boldsymbol{x}}$, where $\boldsymbol{r}^C(t) = h(t)\,\boldsymbol{e}_2 - e\boldsymbol{b}_1(t)$ so that $h(t)$ describes the plunge degree of freedom (see Fig. 1 for the definition of e). The position vector of the point that represents the VA is given by $\boldsymbol{r}_d(t) = h(t)\,\boldsymbol{e}_2 - \eta b\boldsymbol{b}_1(t) + q\boldsymbol{b}_2$. In contrast, $\check{\boldsymbol{x}} = x_1\boldsymbol{b}_1 + x_2\boldsymbol{b}_2$ is the position vector of the material point in the current configuration with respect to the center of mass.

Let $\boldsymbol{b}_k = \boldsymbol{R}(\alpha)\cdot\boldsymbol{e}_k$, where $\boldsymbol{R}$ indicates the orthogonal tensor that describes the rotation of the surface. Given the fact that in this case $\boldsymbol{R}$ describes $\boldsymbol{e}_3$ rotations, we can see that $\boldsymbol{b}_1 = \cos\alpha\boldsymbol{e}_1 + \sin\alpha\,\boldsymbol{e}_2$ and $\boldsymbol{b}_2 = -\sin\alpha\boldsymbol{e}_1 + \cos\alpha\,\boldsymbol{e}_2$. The velocity and acceleration of the material points of the surface and those of the VA, respectively, are given by:

$$\dot{\boldsymbol{r}} = \dot{\boldsymbol{r}}^C + \boldsymbol{\omega}\times\check{\boldsymbol{x}} \quad \text{and} \quad \ddot{\boldsymbol{r}} = \ddot{\boldsymbol{r}}^C + \dot{\boldsymbol{\omega}}\times\check{\boldsymbol{x}} + \boldsymbol{\omega}\times(\boldsymbol{\omega}\times\check{\boldsymbol{x}}), \tag{1}$$

$$\dot{\boldsymbol{r}}_d = \dot{h}\boldsymbol{e}_2 - \eta b\boldsymbol{\omega}\times\boldsymbol{b}_1 + \dot{q}\boldsymbol{b}_2 + q\boldsymbol{\omega}\times\boldsymbol{b}_2, \tag{2}$$

$$\begin{aligned}\ddot{\boldsymbol{r}}_d = {} & \ddot{h}\boldsymbol{e}_2 - \eta b\dot{\boldsymbol{\omega}}\times\boldsymbol{b}_1 - \eta b\boldsymbol{\omega}\times(\boldsymbol{\omega}\times\boldsymbol{b}_1) + \ddot{q}\boldsymbol{b}_2 + 2\dot{q}\boldsymbol{\omega}\times\boldsymbol{b}_2 \\ & + q\dot{\boldsymbol{\omega}}\times\boldsymbol{b}_2 + q\boldsymbol{\omega}\times(\boldsymbol{\omega}\times\boldsymbol{b}_2)\end{aligned} \tag{3}$$

where $\dot{\boldsymbol{r}}^C = \dot{h}\boldsymbol{e}_2 - e\boldsymbol{\omega}\times\boldsymbol{b}_1$ and $\ddot{\boldsymbol{r}}^C = \ddot{h}\boldsymbol{e}_2 - e\boldsymbol{\omega}(\boldsymbol{\omega}\times\boldsymbol{b}_1) - e\dot{\boldsymbol{\omega}}\times\boldsymbol{b}_1$. Therefore, the time rates of change of linear momentum and angular momentum of the lifting surface are given by:

$$\begin{aligned}\int_{\mathcal{B}}\ddot{\boldsymbol{r}}\rho d\mathcal{A} + \ddot{\boldsymbol{r}}_d m_d = {} & \rho A(\ddot{h}\boldsymbol{e}_2 - e\ddot{\alpha}\boldsymbol{b}_2 + e\dot{\alpha}^2\boldsymbol{b}_1) \\ & + m_d[\ddot{h}\boldsymbol{e}_2 + (\eta b\dot{\alpha}^2 - 2\dot{q}\dot{\alpha} - q\ddot{\alpha})\boldsymbol{b}_1 + (\ddot{q} - \eta b\ddot{\alpha} - q\dot{\alpha}^2)\boldsymbol{b}_2],\end{aligned}$$

$$\begin{aligned}\int_{\mathcal{B}}\boldsymbol{r}\times\ddot{\boldsymbol{r}}\rho d\mathcal{A}\cdot\boldsymbol{e}_3 + (\boldsymbol{r}_d\times m_d\ddot{\boldsymbol{r}}_d)\cdot\boldsymbol{e}_3 = {} & \rho J^C\ddot{\alpha} \\ & + \rho A[-e(\ddot{h} + h\dot{\alpha}^2)\cos\alpha - eh\ddot{\alpha}\sin\alpha + e^2\ddot{\alpha}] \\ & + m_d[-(\eta b\cos\alpha + q\sin\alpha)\ddot{h} + (\eta^2 b^2 - \eta bh\sin\alpha + qh\cos\alpha + q^2)\ddot{\alpha} \\ & + (h\sin\alpha - \eta h)\ddot{q} - (qh\sin\alpha + \eta bh\cos\alpha)\dot{\alpha}^2 + 2\dot{q}\dot{\alpha}q + 2\dot{q}\dot{\alpha}h\cos\alpha]\end{aligned}$$

where $\rho\boldsymbol{J}^C\cdot\dot{\boldsymbol{\omega}} = \rho\boldsymbol{J}^C\,\ddot{\alpha}\boldsymbol{e}_3$ and $\rho\boldsymbol{J}^C$ the mass polar moment of inertia of the lifting surface about the center of mass C. Conversely, the time rate of change of the VA linear momentum is given by:

$$\frac{d(\dot{\boldsymbol{r}}_d m_d)}{dt} = m_d[\ddot{h}\boldsymbol{e}_2 + (\eta b\dot{\alpha}^2 - 2\dot{q}\dot{\alpha} - q\ddot{\alpha})\boldsymbol{b}_1 + (\ddot{q} - \eta b\ddot{\alpha} - q\dot{\alpha}^2)\boldsymbol{b}_2].$$

Thus, the balance laws of linear and angular momentum of the augmented system become:

$$\begin{aligned}\boldsymbol{f} + \boldsymbol{f}^L + \hat{\boldsymbol{n}} = {} & \rho A(\ddot{h}\boldsymbol{e}_2 - e\ddot{\alpha}\boldsymbol{b}_2 + e\dot{\alpha}^2\boldsymbol{b}_1) \\ & + m_d[\ddot{h}\boldsymbol{e}_2 + (\eta b\dot{\alpha}^2 - 2\dot{q}\dot{\alpha} - q\ddot{\alpha})\boldsymbol{b}_1 + (\ddot{q} - \eta b\ddot{\alpha} - q\dot{\alpha}^2)\boldsymbol{b}_2],\end{aligned} \tag{4}$$

$$\begin{aligned}\hat{N}_d &= m_d[\ddot{h}\boldsymbol{e}_2 + (\eta b\dot{\alpha}^2 - 2\dot{q}\dot{\alpha} - q\ddot{\alpha})\boldsymbol{b}_1 + (\ddot{q} - \eta b\ddot{\alpha} - q\dot{\alpha}^2)\boldsymbol{b}_2]\cdot\boldsymbol{b}_2 \\ &= m_d\ddot{h}\cos\alpha + m_d(\ddot{q} - \eta b\ddot{\alpha} - q\dot{\alpha}^2)\end{aligned} \tag{5}$$

$$\begin{aligned}\hat{N}_d &= m_d[\ddot{h}\boldsymbol{e}_2 + (\eta b\dot{\alpha}^2 - 2\dot{q}\dot{\alpha} - q\ddot{\alpha})\boldsymbol{b}_1 + (\ddot{q} - \eta b\ddot{\alpha} - q\dot{\alpha}^2)\boldsymbol{b}_2]\cdot\boldsymbol{b}_2 \\ &= m_d\ddot{h}\cos\alpha + m_d(\ddot{q} - \eta b\ddot{\alpha} - q\dot{\alpha}^2)\end{aligned} \tag{6}$$

where $\boldsymbol{r}^A$ is the position vector of the aerodynamic center in the current configuration. The components of the elastic restoring force $\hat{\boldsymbol{n}}$ and couple $\hat{\boldsymbol{m}}$ acting on the lifting surface can be expressed as $N(t) = \hat{N}(h) = kh + k_3h^3$ and $M(t) = \hat{M}(\alpha) = k_\alpha\alpha + k_3^T\alpha^3$. The constitutive equation for the visco-hysteretic absorber, $\hat{N}_d$, can be written as a direct summation of an elastic part $\hat{N}_d^E$ and a dissipative memory-dependent part $\hat{N}_d^D$ according to $\hat{N}_d = \hat{N}_d^E + \hat{N}_d^D$, where $\hat{N}_d^E = k_dq + k_3^dq^3$. The dissipative part is, in turn, expressed as the summation of a linear viscous term and a purely hysteretic term z, $\hat{N}_d^D = c_d\dot{q} + z$, where the evolution of z is described by the Bouc-Wen first-order differential equation (Bouc, 1967; Lacarbonara and Vestroni, 2003; Wen, 1976).

$$\dot{z} = |k_z - (\gamma + \beta\,\mathrm{sgn}(\dot{q})\,\mathrm{sgn}(z)|z^n|)|\dot{q}|. \tag{7}$$

In Eqs. (4) and (5), $(\boldsymbol{f}, \boldsymbol{c})$ refers to the external resultant force and moment with respect to the center of mass and $(\boldsymbol{f}^L, \boldsymbol{c}^L)$ denote the aerodynamic resultant force (lift and drag resultants) and moment, with respect to the aerodynamic center C^A.

Equations (4-6) are linearized, the incorporation of linear viscosity in the airfoil constitutive laws given by $\hat{N}(h, \dot{h}) = kh + c_h\dot{h}$ and $\hat{M}(\alpha, \dot{\alpha}) = k_\alpha\alpha + c_\alpha\dot{\alpha}$. At the same time, full nonlinearity is kept in the visco-hysteretic constitutive law for the VA. The ensuing equations are:

$$\rho A\ddot{h} - \rho Ae\ddot{\alpha} + m_d(\ddot{h} + \ddot{q} - \eta b\ddot{\alpha}) + c_h\dot{h} + kh = (\boldsymbol{f} + \boldsymbol{f}^L)\cdot\boldsymbol{e}_2, \tag{8}$$

$$\rho J^E\ddot{\alpha} - \rho Ae\ddot{h} - m_d\eta b\ddot{h} - m_d\eta b\ddot{q} + J_d^E\ddot{\alpha} + c_\alpha\dot{\alpha} + k_\alpha\alpha = c + ef + c^E, \tag{9}$$

$$m_d(\ddot{h} + \ddot{q} - \eta b\ddot{\alpha}) + c_d\dot{q} + k_dq + z = 0, \tag{10}$$

$$\dot{z} = |k_z - (\gamma + \beta \operatorname{sgn}(\dot{q}) \operatorname{sgn}(z) |z^n| |\dot{q} \tag{11}$$

where $\rho J^E := \rho J^C + \rho A e^2$ and $J_d^E := m_d(\eta b)^2$ denote the polar mass moment of inertia with respect to the elastic center C^E of the wing and of the VA, respectively, while $c^E := df^L + c^L$ is the aerodynamic moment reduced to the elastic center.

According to Glauert's theory of thin airfoils (Glauert, 1947), to obtain the aerodynamic forces induced by a uniform airstream of velocity $V\mathbf{e}_1$ (with zero initial angle of attack), the effective angle of attack is first expressed as:

$$\alpha^{eff} = \alpha + \frac{\dot{\alpha}}{V}(\frac{1}{2} - a)b - \frac{\dot{h}}{V}. \tag{12}$$

The lift force and aerodynamic moment, reduced to the aerodynamic center, are given by:

$$\boldsymbol{f}^L \cdot \boldsymbol{e}_2 = \rho^a b s V^2 C_L, C_L = \left.\frac{dC_L}{d\alpha}\right|_0 \alpha^{eff} = C_L^\alpha \alpha^{eff}, \tag{13}$$

$$c^E = \rho^a b^2 s V^2 C_M, C_M = C_L(\frac{1}{2} + a) + 2C_M^\alpha \tag{14}$$

where s is the wing span, ρ^a is the fluid density, and $C_M^\alpha = 0$ for symmetric airfoils.

Therefore, the equations of motion, as a result of neglecting other kinds of external forces and considering only the linearized parts of the inertial and aerodynamic forces, become:

$$\rho A\ddot{h} - \rho A e\ddot{\alpha} + m_d(\ddot{h} + \ddot{q} - \eta b\ddot{\alpha}) + c_h\dot{h} + kh = \rho^a b s V^2 C_L^\alpha [\alpha + \frac{\dot{\alpha}}{V}(\frac{1}{2} - a)b - \frac{\dot{h}}{V}|, \tag{15}$$

$$\rho J^P\ddot{\alpha} - (\rho A e + m_d\eta b)\ddot{h} - m_d\eta b\ddot{q} + J_\beta^E\ddot{\alpha} + c_\alpha\dot{\alpha} + k_\alpha\alpha = \rho^a b^2 s V^2 C_L^\alpha (\frac{1}{2} + a)[\alpha + \frac{\dot{\alpha}}{V}(\frac{1}{2} - a)b - \frac{\dot{h}}{V}|. \tag{16}$$

$$m_d(\ddot{h} + \ddot{q} - \eta b\ddot{\alpha}) + c_d\dot{q} + k_d q + z = 0, \tag{17}$$

$$\dot{z} = [k_z - (\gamma + \beta \operatorname{sgn}(\dot{q}) \operatorname{sgn}(z) |z^n| |\dot{q}. \tag{18}$$

The dimensional constitutive parameters of the visco-hysteretic VA are denoted by (k_d, k_z, c_d, β, γ, n).

The next few paragraphs illustrate the non-dimensional form of the equations of motion of the augmented aeroelastic system. This form can be arrived at by dividing the vertical coordinate h by b (i.e., the non-dimensional plunge degree of freedom becomes $\bar{h} := h/b$), the VA degree of freedom q by b (i.e., $\bar{q} := q/b$), the hysteretic variable z by $z_0 := k_d b$, and introducing the characteristic time $1/\omega_\alpha$(i.e., $\omega_\alpha := \sqrt{k_\alpha / \rho J^E}$ denotes the torsional frequency of the airfoil). As a result of these steps, the following non-dimensional form of the equations of motion can be obtained:

$$(1+\mu)\ddot{\bar{h}} - (\varepsilon + \mu\eta)\ddot{\alpha} + \mu\ddot{q} + 2\zeta_h\bar{\omega}_h\dot{\bar{h}} + \bar{\omega}_h^2\bar{h} = k_u\bar{V}^2|\alpha + \frac{\dot{\alpha}}{\bar{V}}(\frac{1}{2} - a) - \frac{\dot{\bar{h}}}{\bar{V}}|, \tag{19}$$

$$(r^2 + \mu\eta^2)\ddot{\alpha} - (\varepsilon + \mu\eta)\ddot{\bar{h}} - \mu\eta\ddot{q} + 2r^2\zeta_\alpha\dot{\alpha} + r^2\alpha = k_u\bar{V}^2(\frac{1}{2} + a)|\alpha + \frac{\dot{\alpha}}{\bar{V}}(\frac{1}{2} - a) - \frac{\dot{\bar{h}}}{\bar{V}}|, \tag{20}$$

$$\mu\ddot{\bar{h}} + \mu\ddot{q} - \mu\eta\ddot{\alpha} + \mu\bar{\omega}_d^2[\delta q + (1-\delta)z] + 2(\zeta_d\mu\sqrt{\delta}\bar{\omega}_d)\dot{q} = 0, \tag{21}$$

$$\dot{z} = [1 - (\bar{\gamma} + \bar{\beta} \operatorname{sgn}(\dot{q}) \operatorname{sgn}(z) |z^n| |\dot{q}. \tag{22}$$

where the overbar is dropped in respect to h and the dot over h indicates differentiation with respect to non-dimensional time $\bar{t} := t\omega_\alpha$. The most important non-dimensional parameter in the design of the VA is the mass ratio $\mu := \rho A / m_d$ mμ:= md / ρA로 수식 수정해 주세요 between the VA mass and the wing mass. This parameter is very important because it scales the control force exerted by the VA on the lifting surface.

Given the fact that the plunge frequency is $\omega_h = \sqrt{k / \rho A}$ and the frequency of the VA by itself is $\omega_d = \sqrt{(k_d + k_z) / m_d}$, the following non-dimensional frequencies ratios arise from the non-dimensionalization: $\bar{\omega}_h = \omega_h / \omega_\alpha$ (non-dimensional plunge frequency) and $\bar{\omega}_d = \omega_d / \omega_\alpha$ (non-dimensional VA frequency). The non-dimensional pitch frequency becomes 1 in this case. The mass and elastic distribution properties of the lifting surface are summarized by $r := \sqrt{\rho J^E / (\rho A b^2)}$ and $\varepsilon := e/b$. The non-dimensional damping coefficients of the airfoil are given by: $\zeta_h := c_h / (2\rho A\omega_h)$, $\zeta_\alpha := c_\alpha / (2\rho J^E\omega_\alpha)$. In contrast, the remaining non-dimensional constitutive parameters of the visco-hysteretic VA (besides $\bar{\omega}_d$) can be expressed as: $\zeta_d := c_d / 2m_d\sqrt{m_d / k_d}$, $\bar{\gamma} := \gamma b(z_0)^{n-1}$, $\bar{\beta} := \beta b(z_0)^{n-1}$, and $\delta := k_d / (k_d + k_z)$.

The non-dimensional velocity is $\bar{V} := V(b\omega_\alpha)$ and the aerodynamic constant is given by $k_u := \rho s b^2 C_L^0 / \rho A$.

3. Design and Performance of the Aeroelastic Visco-hysteretic VA

The well-known Den Hartog visco-elastic VA (Den Hartog, 1934; Frahm, 1911) is widely regarded as effective for vibration cosntrol of a mechanical system subject to a harmonic time-varying force. This effectiveness is attributed to the anti-resonance phenomenon, which completely cancels the response when the system and the VA are undamped and the frequency of the VA is exactly tuned to the frequency of

Table 1. Dimensional wing model parameters

Parameters of the two-dof wing model	
ρ^a	$1.225\ kg \cdot m^{-3}$
b	$0.135\ m$
s	$1\ m^2$
k	$2844.4\ N \cdot m$
k_α	$(2.82 - 62.332\alpha + 3709.71\alpha^2)\ N \cdot m$
c_h	$27.43\ N \cdot s \cdot m^{-1}$
c_α	$0.036\ N \cdot s \cdot m$
ρA	$12.387\ kg$
J^E	$0.065\ kg \cdot m^2$
C_L^o	6.28

Table 2. Non-dimensional wing model parameters

Non-dimensional wing parameters	
a	–0.4
$\bar{\omega}_h$	0.3875
ε	0.0467
r	0.5366
ζ_h	0.0731
ζ_α	0.0071
k_u	0.0113
$\eta = 1/2 - a$	0.9

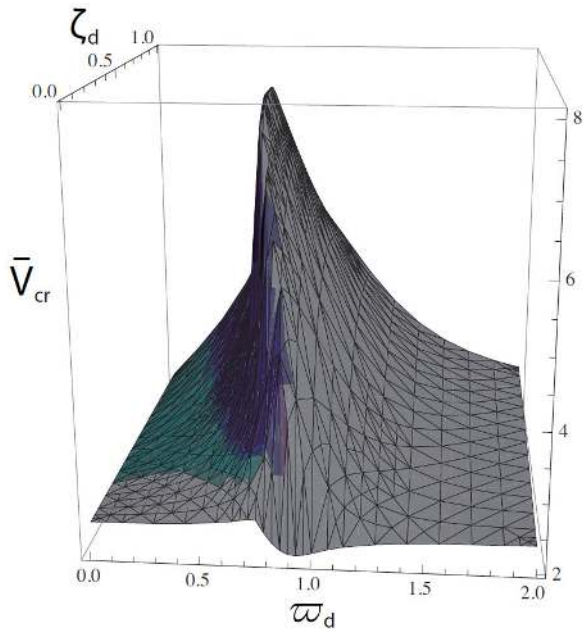

Fig. 2. Variation of the flutter velocity $\bar{V}_{cr}$ of the augmented three-dof system, comprising the linear visco-elastic vibration absorber with $\bar{\omega}_d$ and ζ_d as obtained by the Routh-Hurwitz criterion.

the system driven to resonance. There is no exact resonance cancellation when the structure is damped, while the anti-resonance phenomenon, accompanied by small amplitudes, is exhibited provided that the VA frequency is properly tuned to the frequency of the damped system.

Eight parameters must be determined to facilitate the design of a visco-hysteretic VA for flutter and post-flutter control. These parameters are the mass ratio μ, the position of the VA along the wing's chord-wise direction η, the VA frequency $\bar{\omega}_d$, which arises from the tuning condition of the VA's overall stiffness, the VA damping ratio ζ_d, and the other constitutive parameters of the hysteretic part of the VA restoring force, namely, (δ, n, $\bar{\beta}$, $\bar{\gamma}$).

When the hysteretic part of the restoring force z is discarded, the (dimensional) frequency of the VA can be expressed as $\omega^E = \sqrt{k_d / m_d} = \sqrt{\delta}\,\omega_d$. While ω_d represents the linear frequency of the VA (i.e., at infinitesimal oscillation amplitudes), the nonlinear stiffness variations of the hysteretic VA during its finite cycles are such that its (nonlinear) frequency scales with ω^E, whose non-dimensional counterpart, ω^E / ω_d turns out to be $\sqrt{\delta}\,\omega_d$. During flutter, it is expected that the VA will oscillate together with the appropriately phased airfoil so as to introduce additional damping into the augmented system.

A rational design of the VA consists of requiring ω^E to be equal to the flutter frequency. This tuning condition serves as a good initial guess for the optimization process, which results in the optimum tuning. Once the flutter speed of the system without VA is calculated employing the Routh-Hurwitz criterion (Meirovitch, 1970), the frequency of the flutter mode can be computed accordingly.

The mass ratio μ and the VA position described by η must satisfy certain physical restrictions. The weight limitation on the wing is such that the value of μ can be as high as 1/100 (an upper bound for the VA mass), while placing the VA at three-quarters of the chord toward the trailing edge leads to $\eta = \frac{1}{2} - a$. These restrictions represent limitations on the magnitude of the control force. This force is greatly enhanced by higher mass ratios and by a position closer to the tip of the wing's trailing edge, where the torsional couple exerted by the VA on the wing profile is maximized.

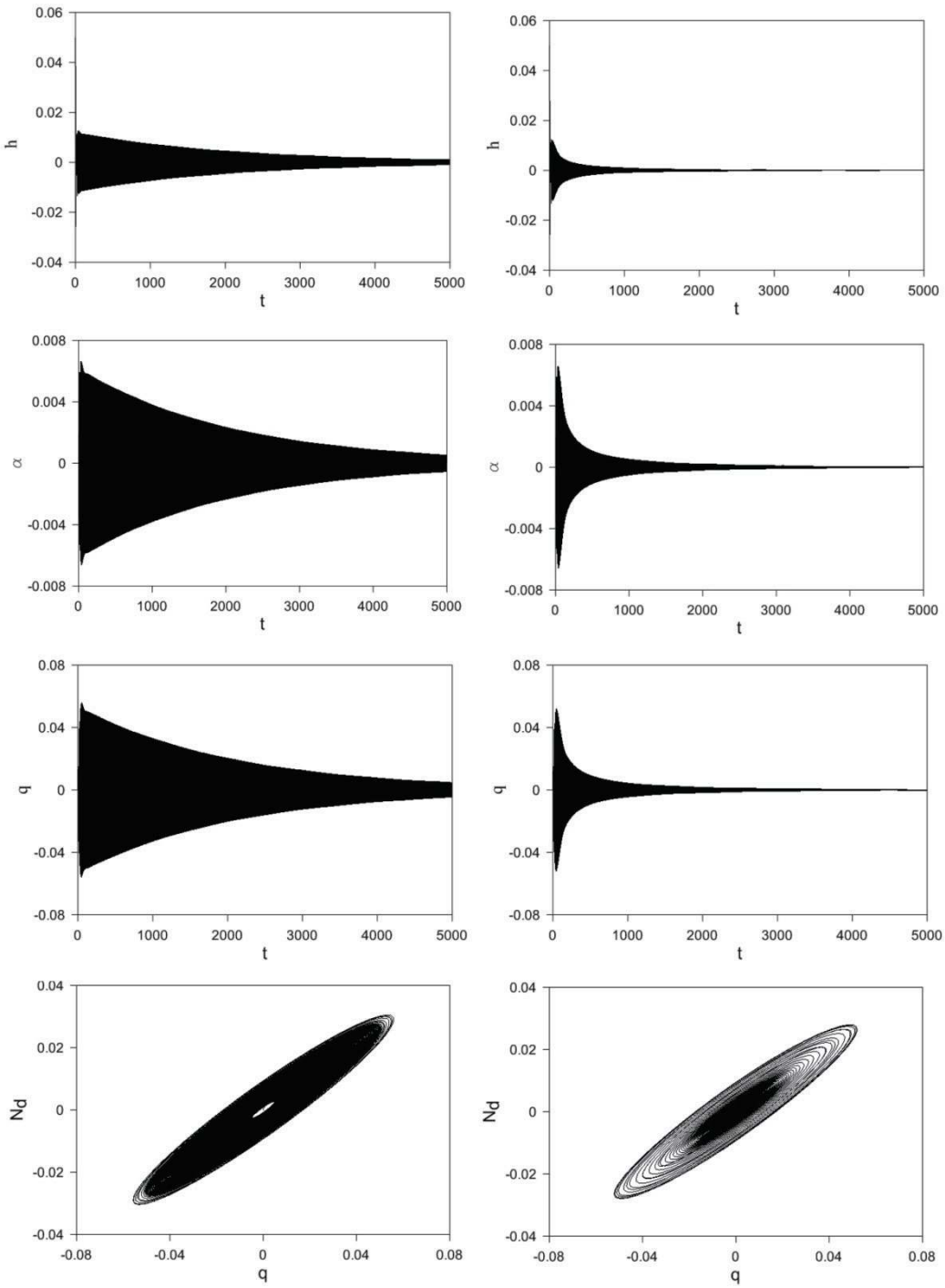

Fig. 3. From left to right: (first line) time history of h, (second line) time history of α, (third line) time history of q, (bottom) loops of the total vibration absorber (VA) force, given respectively by $N_d = 2\zeta_d\sqrt{\delta}\,\bar{\omega}_d\dot{q}$ and $N_d = \bar{\omega}_d^2[\delta q + (1\text{-}\delta)z]+2\zeta_d\sqrt{\delta}\,\bar{\omega}_d\dot{q}$ in $\bar{t}\in[0,5000]$ for the three-dof system with the linear visco-elastic VA (left) and with the visco-hysteretic VA (right). The flow velocity is $\bar{V} = 0.999\ \bar{V}_{cr}$.

In relation to the VA damping ratio ζ_d, an optimum damping ratio can increase the flutter speed by orders of magnitude, while the hysteretic part of the force does not influence the onset of flutter. Hysteresis is shown to have a fundamental role in increasing the decay rates of the transients. This occurs mostly in the pre-flutter regime, but is also seen in the post-flutter regime.

By adopting the parameters of the wing model studied

DOI:10.5139/IJASS.2011.12.4.331

by Behal et al. (2006), the application of the Routh-Hurwitz criterion leads to calculation of the non-dimensional linear flutter speed of the airfoil by itself found to be $\bar{V}_{cr} = 2.46$. The model in question is shown in Tables 1 and 2.

The optimal parameters for the linear visco-elastic VA can be determined by a numerical search calculating the flutter speed via the Routh-Hurwitz criterion on a grid that discretizes the parameter plane $(\bar{\omega}_d, \zeta_d)$ in a lattice. Figure 2 shows the results of these computations, which lead to the following optimal parameters: $\bar{\omega}_d = 0.72$ and $\zeta_d = 0.36$. With these optimal parameters, the flutter speed goes up to 8.3; an increase of approximately 240 percent. The sensitivity of the flutter speed with respect to $\bar{\omega}_d$ and ζ_d can be appreciated by computing the flutter speed at meaningful values detuned from the optimal values. For example, if the VA frequency is tuned with the frequency of the flutter mode, $\bar{\omega}_d = 1$, and if the damping ratio is set to $\zeta_d = 0.1$, flutter speed is determined to be 4.5 and the increase with respect to the case without VA is only 83 per cent. In contrast, if $\bar{\omega}_d = 0.87$ and $\zeta_d = 0.1$, the flutter speed goes up to 5.9, with an increase of approximately 140 per cent.

Numerical investigations via integration of the equations of motion into the effects of the visco-hysteretic VA (i.e., the parallel arrangement of a dashpot and a Bouc-Wen element) have shown that the purely hysteretic part of a system is unable to alter the flutter boundary of a system endowed with a purely visco-elastic VA. However, it does increase the effective damping of the system in the pre-flutter regime, as shown in Fig. 3. The decay rate of the airfoil response to initial conditions is greatly enhanced by hysteresis. Moreover, the decay rate increases with the magnitude of the initial conditions up to a certain threshold, at which the effective damping is maximized.

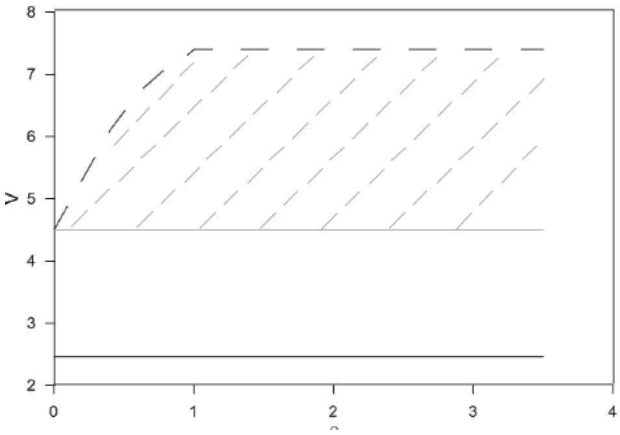

Fig. 4. Variation of the flutter speed with the hysteretic constitutive parameter $\bar{\beta}$ with the vibration absorber (VA, thin solid line) and without the VA (thick solid line), when $\zeta_d = 0.1$ while the other parameters are fixed to $\delta = 0.2$, $n = 1$, $\bar{\omega}_d = 1$, and $\bar{\gamma} = \bar{\beta}$. The shaded region represents the post-flutter range, where the lifting surface exhibits limit-cycle oscillations due to the nonlinear hysteretic force in the VA. The boundary is defined as the speed at which the torsional angle reaches the threshold amplitude of 0.2 rad, beyond which the response diverges.

It is interesting to study the effects of detuning in the optimal parameters of the visco-elastic VA while observing the effects of variations of the constitutive parameters of the hysteretic part of the VA restoring force. For example, in Fig. 4 the visco-elastic parameters are set to $\bar{\omega}_d = 1$ and $\zeta_d = 0.1$. In such a case, flutter is reached at a flow speed of 4.5, with an increase with respect to the system without VA of only 83 per cent. However, in this detuned case there is a post-flutter range in which the airfoil exhibits LCOs with relatively small amplitudes. Hence, the hysteresis has a twofold effect: it enhances damping in the pre-flutter stage and controls the post-flutter up to a threshold value of the speed beyond which the response of the airfoil diverges if all other structural /aerodynamic nonlinearities are neglected. Some examples of such post-flutter responses are shown in Figs. 5-7 at various flow speeds when $\bar{\gamma} = 1 = \bar{\beta}$.

To assess the effects of the purely hysteretic component of the VA restoring force, the dashpot contribution is neglected and a set of post-flutter responses are shown in Figs. 8-10 with $\bar{\gamma} = 1 = \bar{\beta}$ at various flow speeds. While in the immediate vicinity of flutter, the LCO has one dominant frequency (the nonlinear flutter frequency); multiple harmonics of the flutter frequency are manifested at speeds further away from the flutter condition. More interestingly, when the flow speed is 3.66 times the flutter speed, the LCO undergoes a Hopf bifurcation by which the post-critical LCO becomes amplitude-modulated (i.e., quasiperiodic motion), as shown in Fig. 10.

4. Discussion and Conclusions

In this paper, a visco-hysteretic VA is proposed in order to enhance the aeroelastic stability of an airfoil by increasing its flutter speed. The passive system is a parallel arrangement of a dashpot and a rate-independent hysteretic element, represented by the Bouc-Wen differential model (Bouc, 1967; Lacarbonara and Vestroni, 2003; Wen, 1976).

This paper shows that, for a set of parameters representing an experimental airfoil (Behal et al., 2006), the optimized purely visco-elastic VA (without the hysteretic element) can result in an increase of the flutter speed by up to 240 per cent when the mass ratio is 1 per cent. Numerical investigations are carried out into the effects of the purely hysteretic VA, i.e. a VA without the dashpot. These results show that a purely

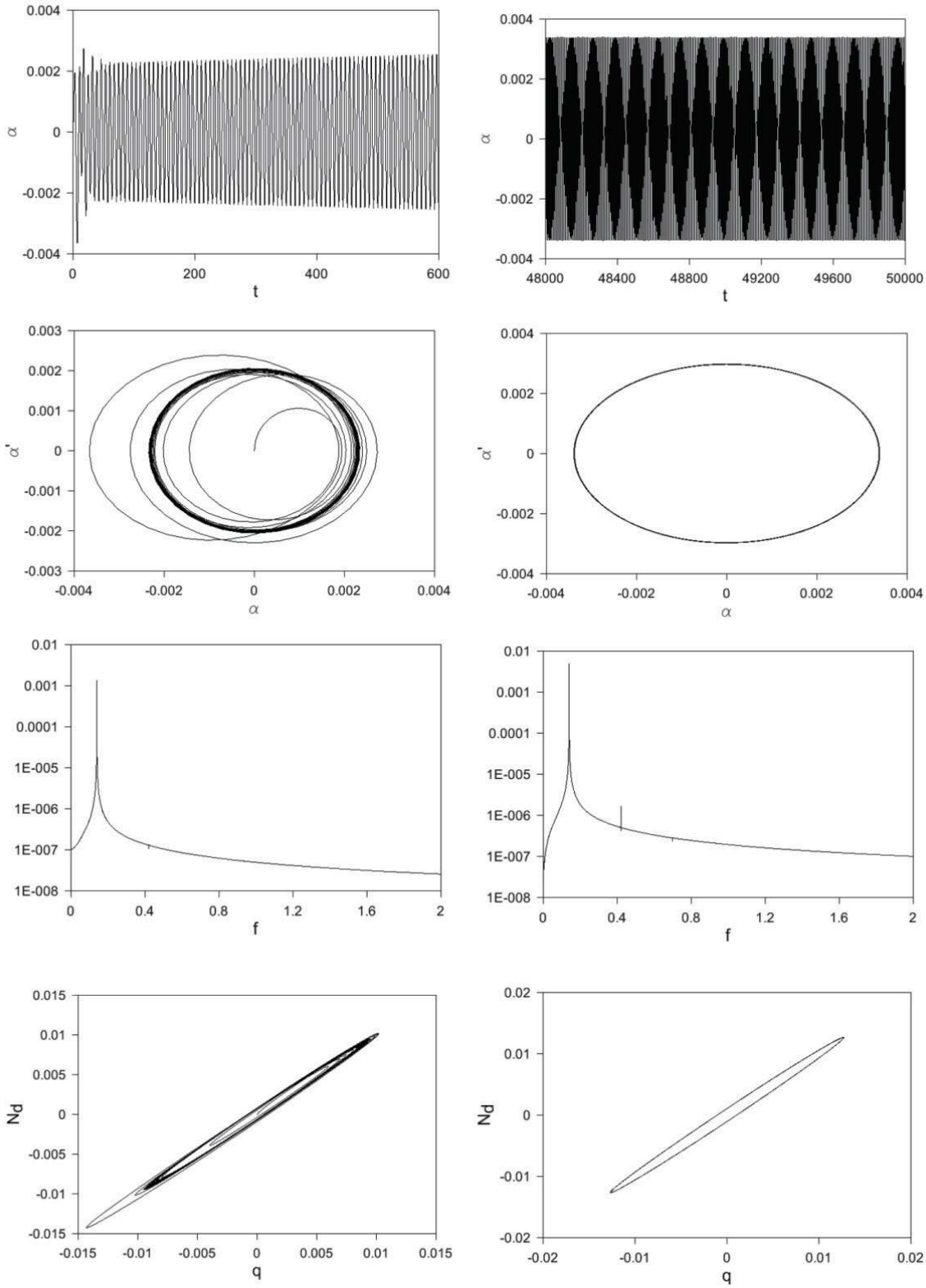

Fig. 5. From left to right: (top) time history of α and phase diagrams (α, $\dot{\alpha}$) in the transient phase ($\bar{t}\in[0,600]$ and $\bar{t}\in[0,200]$, respectively) and at steady state ($\bar{t}\in[4.8\cdot10^4, 5\cdot10^4]$ and $\bar{t}\in[3\cdot10^4, 5\cdot10^4]$, respectively), (middle) Fast Fourier Transform (FFT) of α and q, (bottom) loops of total vibration absorber force $N_d = \bar{\omega}_d^2[\delta q + (1\text{-}\delta)z]+2\zeta_d\sqrt{\delta}\,\bar{\omega}_d\dot{q}$ in the transient phase ($\bar{t}\in[0,600]$) and at steady state ($\bar{t}\in[3\cdot10^4, 5\cdot10^4]$), when ζ_d= 0.1 and $\bar{V}$ = 1.02 $\bar{V}_{cr}$ with $\bar{V}_{cr}$ = 4.5. The peak in the FFT is attained by $\bar{f}$ = 0.14, where $\bar{f}$ denotes the non-dimensional frequency.

DOI:10.5139/IJASS.2011.12.4.331

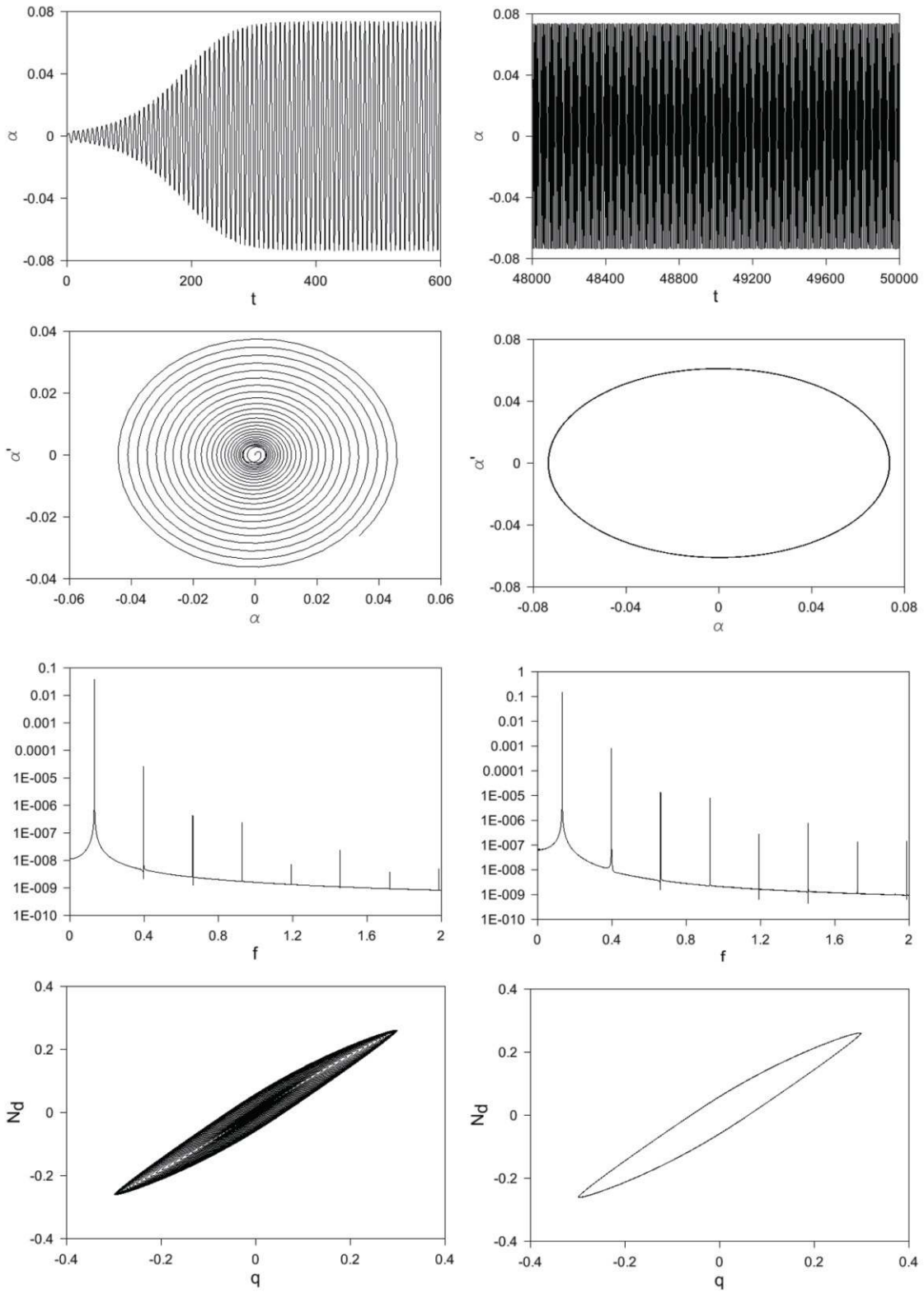

Fig. 6. From left to right: (top) time history of α and phase diagrams (α, $\dot{\alpha}$) in the transient phase ($\bar{t}\in[0,600]$ and $\bar{t}\in[0,200]$, respectively) and at steady state ($\bar{t}\in[4.8\cdot10^4, 5\cdot10^4]$ and $\bar{t}\in[3\cdot10^4, 5\cdot10^4]$, respectively) (middle) FFT of α and q, (bottom) loops of total vibration absorber force in the transient phase ($\bar{t}\in[0,600]$) and at steady state ($\bar{t}\in[3\cdot10^4, 5\cdot10^4]$), when $\zeta_d = 0.1$ and $\bar{V}= 1.33\ \bar{V}_{cr}$ with $\bar{V}_{cr} = 4.5$. The peak in the FFT is attained by $\bar{f} = 0.132$.

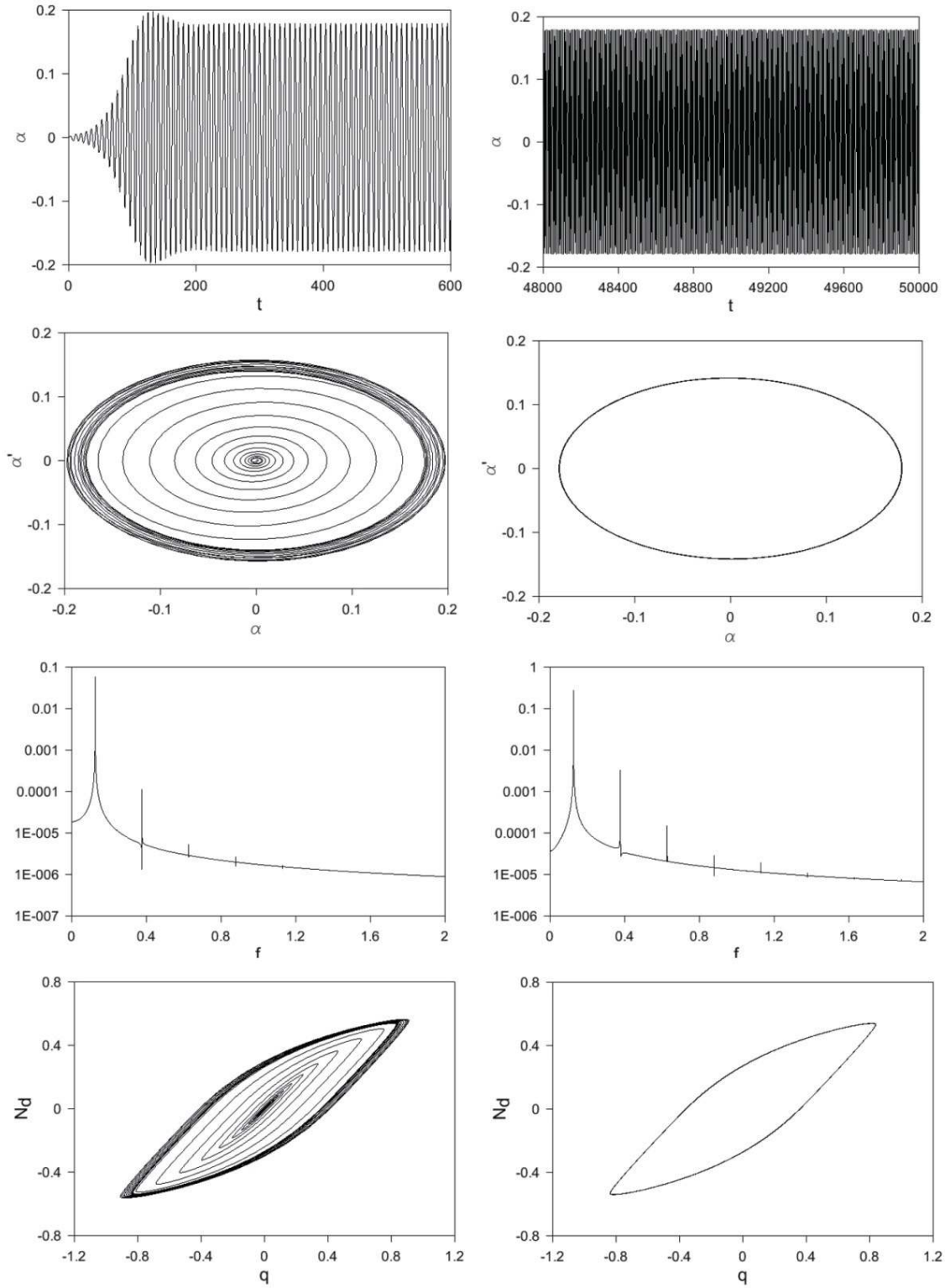

Fig. 7. From left to right: (top) time history of α and phase diagrams (α, $\dot{\alpha}$) in the transient phase ($\bar{t}\in[0,600]$ and $\bar{t}\in[0,200]$, respectively) and at steady state ($\bar{t}\in[4.8\cdot10^4, 5\cdot10^4]$ and $\bar{t}\in[3\cdot10^4, 5\cdot10^4]$, respectively), (middle) FFT of α and q,(bottom) loops of total vibration absorber force in the transient phase ($\bar{t}\in[0,600]$) and at steady state ($\bar{t}\in[3\cdot10^4, 5\cdot10^4]$), when $\zeta_d = 0.1$ and $\bar{V} = 1.64\ \bar{V}_{cr}$ with $\bar{V}_{cr} = 4.5$. The peak in the FFT is attained by $\bar{f} = 0.14$.

DOI:10.5139/IJASS.2011.12.4.331

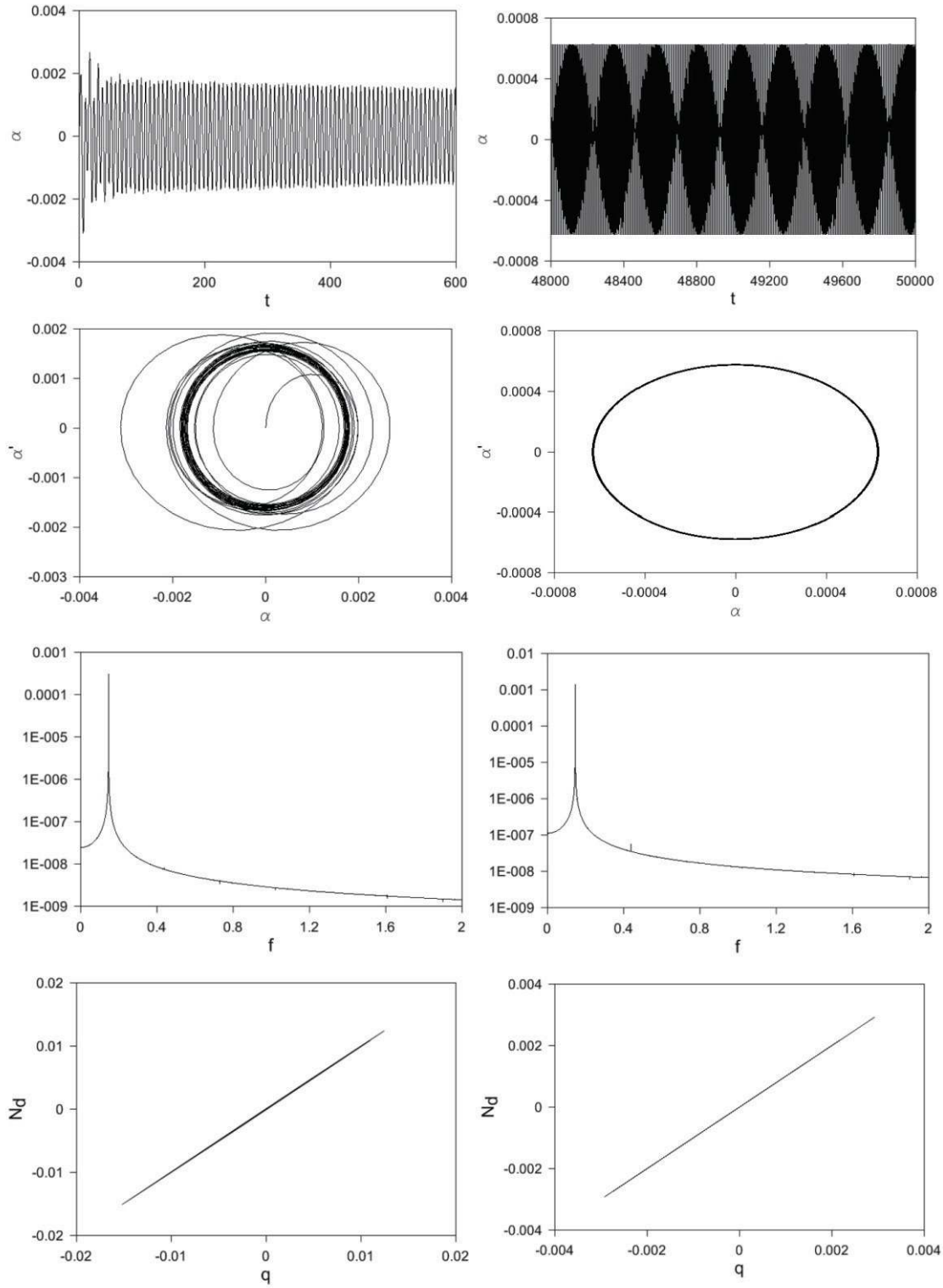

Fig. 8. From left to right: (top) time history of α and phase diagrams (α, $\dot{\alpha}$) in the transient phase ($\bar{t} \in [0,600]$ and $\bar{t} \in [0,200]$, respectively) and at steady state ($\bar{t} \in [4.8 \cdot 10^4, 5 \cdot 10^4]$ and $\bar{t} \in [3 \cdot 10^4, 5 \cdot 10^4]$, respectively), (middle) FFT of α and q,(bottom) loops of total vibration absorber force in the transient phase ($\bar{t} \in [0,600]$) and at steady state ($\bar{t} \in [3 \cdot 10^4, 5 \cdot 10^4]$), when $\zeta_d = 0$ and $\bar{V} = 1.05\ \bar{V}_{cr}$ with $\bar{V}_{cr} = 2.1$. The peak in the FFT is attained by $\bar{f} = 0.146$.

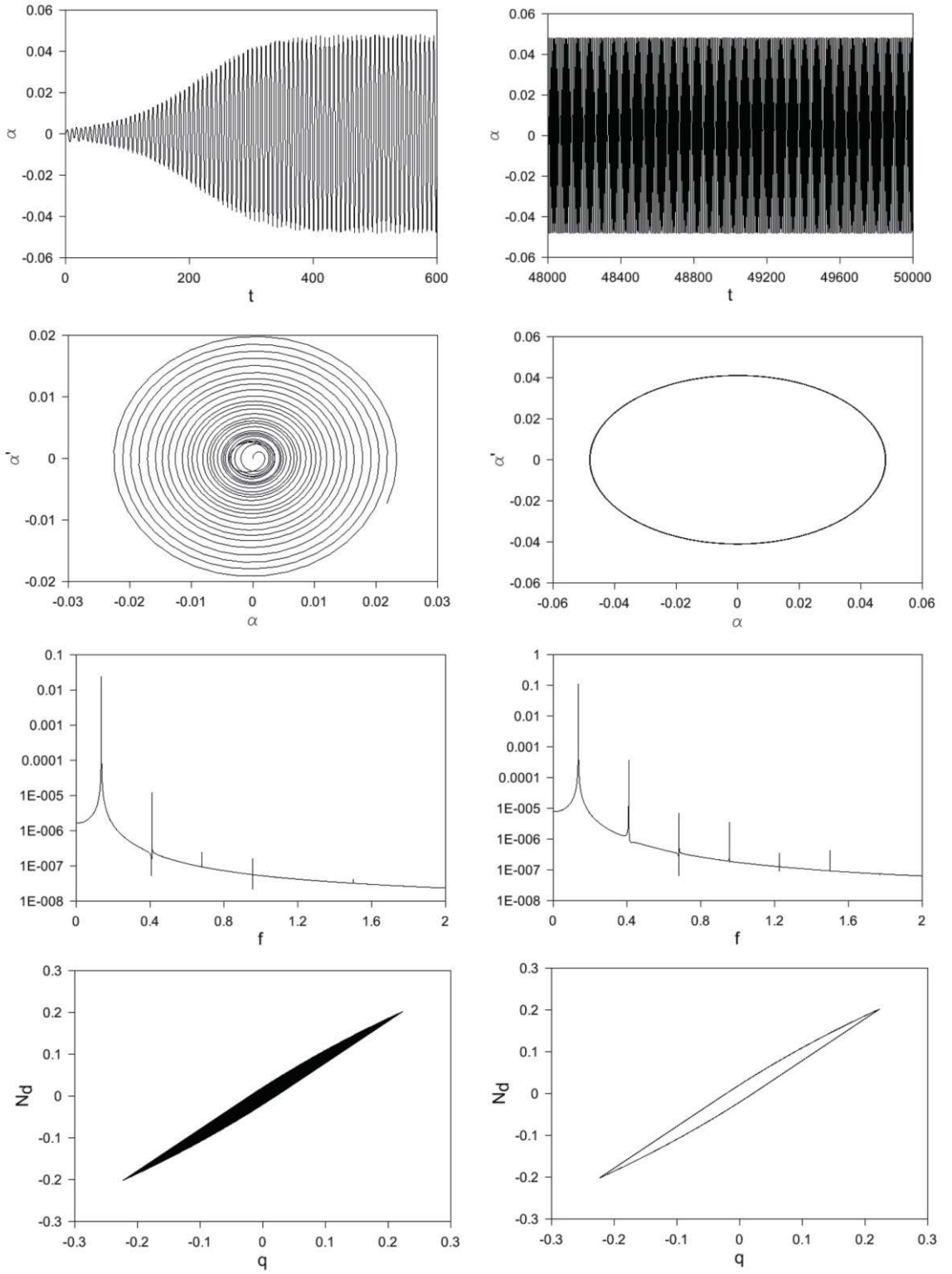

Fig. 9. From left to right: (top) time history of α and phase diagrams (α, $\dot{\alpha}$) in the transient phase ($\bar{t}\in[0,600]$ and $\bar{t}\in[0,200]$, respectively) and at steady state ($\bar{t}\in[4.8\cdot10^4, 5\cdot10^4]$ and $\bar{t}\in[3\cdot10^4, 5\cdot10^4]$, respectively), (middle) FFT of α and q, (bottom) loops of total vibration absorber force $N_d = \bar{\omega}_d^2[\delta q + (1\text{-}\delta)z]$ in the transient phase ($\bar{t}\in[0,600]$) and at steady state ($\bar{t}\in[3\cdot10^4, 5\cdot10^4]$), when $\zeta_d = 0$ and $\bar{V}_{cr} = 2.38\ \bar{V}_{cr}$ with $\bar{V}_{cr} = 2.1$. The peak in the FFT is attained by $\bar{f} = 0.136$.

DOI:10.5139/IJASS.2011.12.4.331

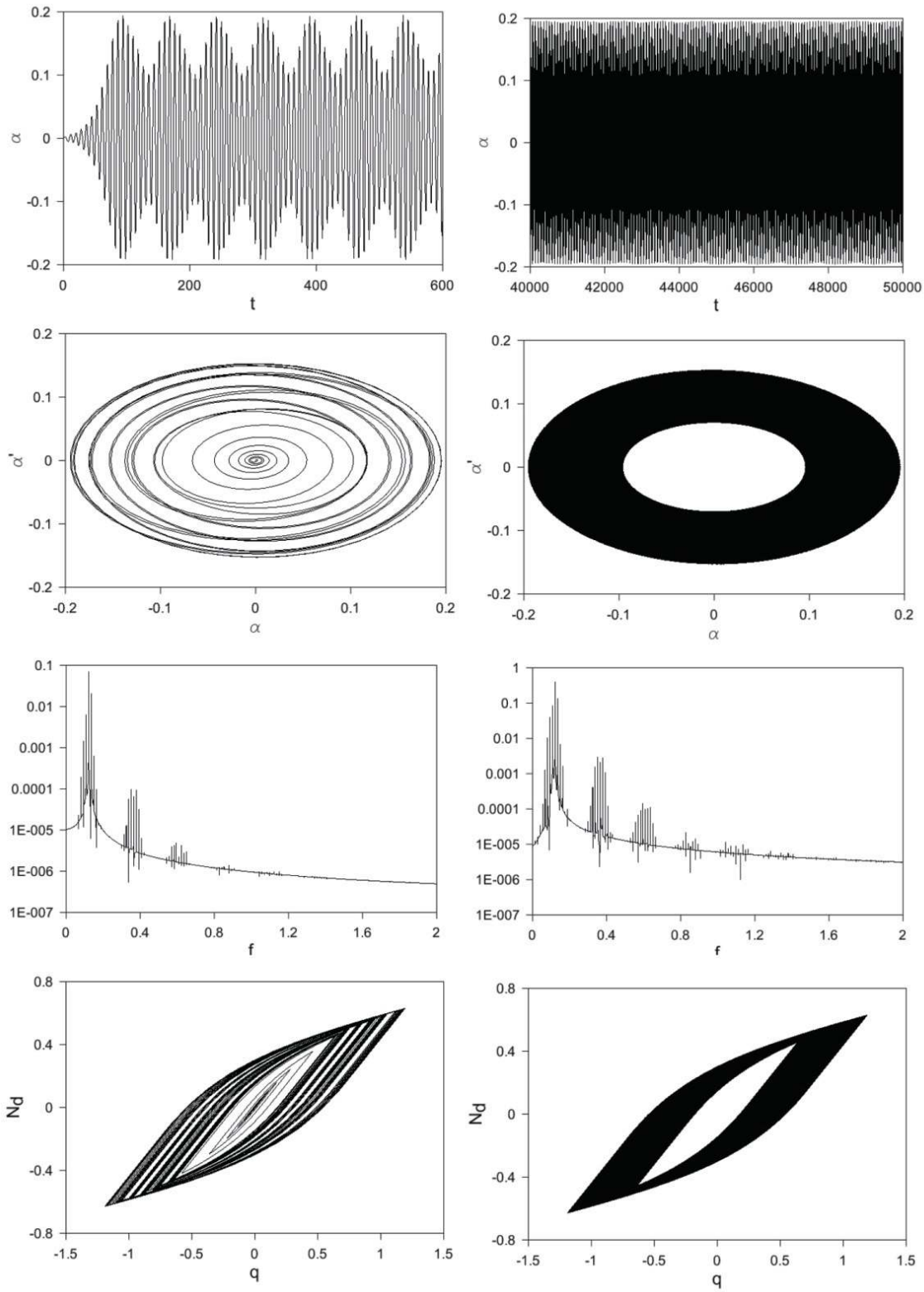

Fig. 10. From left to right: (top) time history of α and phase diagrams (α, $\dot{\alpha}$) in the transient phase ($\bar{t}\in[0,600]$ and $\bar{t}\in[0,200]$, respectively) and at steady state ($\bar{t}\in[4\cdot10^4, 5\cdot10^4]$ and $\bar{t}\in[3\cdot10^4, 5\cdot10^4]$, respectively), (middle) FFT of α and q, (bottom) loops of total vibration absorber force in the transient phase ($\bar{t}\in[0,600]$) and at steady state ($\bar{t}\in[3\cdot10^4, 5\cdot10^4]$), when $\zeta_d = 0$ and $\bar{V} = 3.66\ \bar{V}_{cr}$ with $\bar{V}_{cr} = 2.1$. The peak in the FFT is attained by $\bar{f} = 0.122$.

hysteretic restoring force does not have the capability to change the flutter boundary of the airfoil, since at the onset of flutter the aeroelastic destabilizing forces can only be counteracted by a VA control force in which the resistive component depends on the relative instantaneous velocity. In contrast, the hysteretic restoring force can only dissipate energy over a full cycle of oscillation. However, the presence of a purely hysteretic restoring force enhances damping in the pre-flutter regime and controls the post-flutter behavior over a significant range of flow speeds.

The optimization described in this paper can be carried out in the presence of a visco-hysteretic force by applying the Routh-Hurwitz criterion, accounting for only the linear visco-elastic part of the restoring force. The primary effect of the hysteretic part of the restoring force is to increase the effective damping of the system in the pre-flutter regime, as shown in Fig. 3. In practice, the decay rate of the airfoil response to initial conditions is greatly enhanced by hysteresis. In the optimal configuration of the absorber, decay rates can only be controlled by hysteresis. This justifies its use in conjunction with the linear visco-elasticity of the spring and dashpot. The experimental validation of the control system is part of an ongoing research project.

Acknowledgements

This material is based on work partially supported by FY 2008 MIUR under a PRIN Grant "Shape-memory alloy advanced modeling for industrial and biomedical applications" awarded to WL.

Professor Marzocca from Clarkson University (Potsdam, NY, USA) is gratefully acknowledged for initial discussions on the experimental airfoil used for the computations and for sharing comparisons with the calculations of the flutter condition performed by his research group in earlier works.

References

Behal, A., Marzocca, P., Rao, V. M., and Gnann, A. (2006). Nonlinear adaptive control of an aeroelastic two-dimensional lifting surface. *Journal of Guidance, Control, and Dynamics*, 29, 382-390.

Bouc, R. (1967). Forced vibrations of mechanical systems with hysteresis. *Proceedings of the 4th International Conference on Nonlinear Oscillations*, Prague, Czechoslovakia.

Carpineto, N., Lacarbonara, W., and Vestroni, F. (2010). Hysteresis-based nonlinear vibration absorbers. *Proceedings of the 13th Conference on Nonlinear Vibrations, Dynamics Eurodyn, and Mulitbody Systems*, Blacksburg, VA.

Carpineto, N., Vestroni, F., and Lacarbonara, W. (2011). Vibration mitigation by means of hysteretic tuned mass dampers. *Proceedings of the 8th International Conference on Structural Dynamics*, Leuven, Belgium.

Den Hartog, J. P. (1934). *Mechanical Vibrations*. New York: McGraw-Hill.

Frahm, H. (1911). Device for Damping Vibration of Bodies. US Patent No. 989958.

Glauert, H. (1947). *The Elements of Aerofoil and Airscrew Theory*. 2nd ed. New York: Cambridge University Press.

Hu, J. L. and Zhou, L. (2007). Semi-active flutter control of a high-aspect-ratio wing using multiple MR dampers. *Proceedings of the Conference on Sensors and Smart Structures Technologies for Civil, Mechanical, and Aerospace Systems*, San Diego, CA.

Lacarbonara, W. and Vestroni, F. (2003). Nonclassical responses of oscillators with hysteresis. *Nonlinear Dynamics*, 32, 235-258.

Lee, Y. S., Kerschen, G., Michael McFarland, D., Joel Hill, W., Nichkawde, C., Strganac, T. W., Bergman, L. A., and Vakakis, A. F. (2007a). Suppressing aeroelastic instability using broadband passive targeted energy transfers, part 2: experiments. *AIAA Journal*, 45, 2391-2400.

Lee, Y. S., Vakakis, A. F., Bergman, L. A., McFarland, D. M., and Kerschen, G. (2007b). Suppressing aeroelastic instability using broadband passive targeted energy transfers, part 1: theory. *AIAA Journal*, 45, 693-711.

Marzocca, P., Librescu, L., and Silva, W. A. (2002). Flutter, postflutter, and control of a supersonic wing section. *Journal of Guidance, Control, and Dynamics*, 25, 962-970.

McGowan, A. M. R. (1999). Feasibility study on using shunted piezoelectrics to reduce aeroelastic response. *Proceedings of SPIE*, 3674, 178-195.

Meirovitch, L. (1970). *Methods of Analytical Dynamics*. New York: McGraw-Hill.

Njuguna, J. (2007). Flutter prediction, suppression and control in aircraft composite wings as a design prerequisite: A survey. *Structural Control and Health Monitoring*, 14, 715-758.

Reed, W. H., Cazier, F. W., and Foughner, J. T. (1980). Passive Control of Wing/Store Flutter. NASA Technical Memorandum 81865. Washington, DC: National Aeronautics and Space Administration.

Richard, R. E. and Clark, R. L. (2003). Delta wing flutter control using spatially optimized transducers. *Journal of Intelligent Material Systems and Structures*, 14, 677-691.

Rocha, J., Moniz, P., and Suleman, A. (2007). Aeroelastic control of a wing with active skins using piezoelectric patches. *Mechanics of Advanced Materials and Structures*, 14, 23-32.

Schweiger, J., Simpson, J., Weiss, F., Coetzee, E., and Boller, C. (1999). Needs for the analysis and integrated design optimization of active and passive structure for active aeroelastic wings. *Proceedings of SPIE*, 3668, 117-130.

Vestroni, F., Lacarbonara, W., and Carpineto, N. (2011). Hysteretic Tuned Mass Damper for Passive Control of Mechanical Vibrations. Italy Patent No. RM2011A000434.

Wen, Y. K. (1976). Method for random vibration of hysteretic systems. *Journal of the Engineering Mechanics*-ASCE, 102, 249-263.